ELSEVIER

Journal of Structural Geology 29 (2007) 1744–1756

JOURNAL OF STRUCTURAL GEOLOGY

www.elsevier.com/locate/jsg

Fold origin of the NE-lobe of the Sudbury Basin, Canada: Evidence from heterogeneous fabric development in the Onaping Formation and the Sudbury Igneous Complex

Christian Klimczak [a], Andrea Wittek [a], Daniel Doman [b], Ulrich Riller [b,*]

[a] *Freie Universität Berlin, Malteserstrasse 74-100, 12249 Berlin, Germany*
[b] *Museum für Naturkunde, Humboldt Universität zu Berlin, Invalidenstrasse 43, 10115 Berlin, Germany*

Received 10 June 2007; received in revised form 31 August 2007; accepted 4 September 2007
Available online 23 September 2007

Abstract

Structural analysis of the Onaping Formation, a heterolithic impact melt breccia, and the Granophyre in the NE-lobe of the 1.85 Ga Sudbury Igneous Complex (SIC) assist in understanding the formation of the Sudbury Basin. Previously, the lack of mesoscopic strain fabrics in the SIC, in contrast to pervasive fabrics in the Onaping Formation of the NE-lobe, led to interpretations of the shape of the NE-lobe as primary. We demonstrate that the structures of the Onaping Formation are consistent with deformation in a fold core controlled by the mechanically stronger Granophyre of the NE-lobe. Evidence for this interpretation includes the (1) presence of open structural domes and basins, (2) geometry of planar mineral shape fabrics, (3) variation in shape fabric intensity, and (4) kinematics of prominent faults. Folding of the Onaping Formation affected the SIC because fold geometry is based on dip data in the SIC and fold-related faults cut both the Onaping Formation and Granophyre. Microstructural observations point to different temperatures during deformation in both units that are consistent with initiation of folding during cooling of the SIC upon reaching middle greenschist-facies metamorphic conditions.

Keywords: Sudbury Basin; Heterogeneous deformation; Folds; Faults; Mineral fabrics

1. Introduction

With an estimated diameter of 200–250 km, the Sudbury impact structure, in the southern Canadian Precambrian Shield (Fig. 1), is the second largest impact structure known on Earth (Grieve et al., 1991; Deutsch et al., 1995; Spray et al., 2004). The central portion of the impact structure is marked by the synformal and layered Main Mass of the Sudbury Igneous Complex (henceforth called SIC) that is 1.85 Ga in age (Krogh et al., 1982, 1984). Along with the overlying Onaping Formation, a heterolithic impact melt breccia, and post-impact sedimentary rocks, the SIC forms the 60 km by 30 km Sudbury Basin (Brocoum and Dalziel, 1974). To the north and east, the SIC rests on granitoid, gneissic and granulite rocks, notably the Levack Gneiss Complex, of the Archean Superior Province (Fig. 1). To the south, it overlies steeply northward-dipping and overturned metasedimentary and metavolcanic strata of the Paleoproterozoic Huronian Supergroup. These rocks were deformed by the ca. 2.4–2.2 Ga Blezardian and ca. 1.9–1.8 Ga Penokean episodes of orogenic deformation (Riller and Schwerdtner, 1997; Riller et al., 1999), the latter one of which affected also the SIC and its overlying rocks.

The SIC is widely accepted to be the relic of a solidified impact melt sheet (Grieve et al., 1991; Deutsch et al., 1995) formed by shock-induced fusion of Archean and Paleoproterozoic target rocks based on the presence of massive pseudotachylitic breccia, shatter cones and planar deformation features (e.g., Bray et al., 1966; Dressler, 1984b; Spray and Thompson, 1995). Upon cooling, the melt sheet differentiated into, what is traditionally known as, the Norite, Quartz-gabbro and

* Corresponding author. Tel.: +49 30 2093 8573; fax: +49 30 2093 8565.
E-mail address: ulrich.riller@museum.hu-berlin.de (U. Riller).

0191-8141/$ - see front matter © 2007 Elsevier Ltd. All rights reserved.
doi:10.1016/j.jsg.2007.09.003

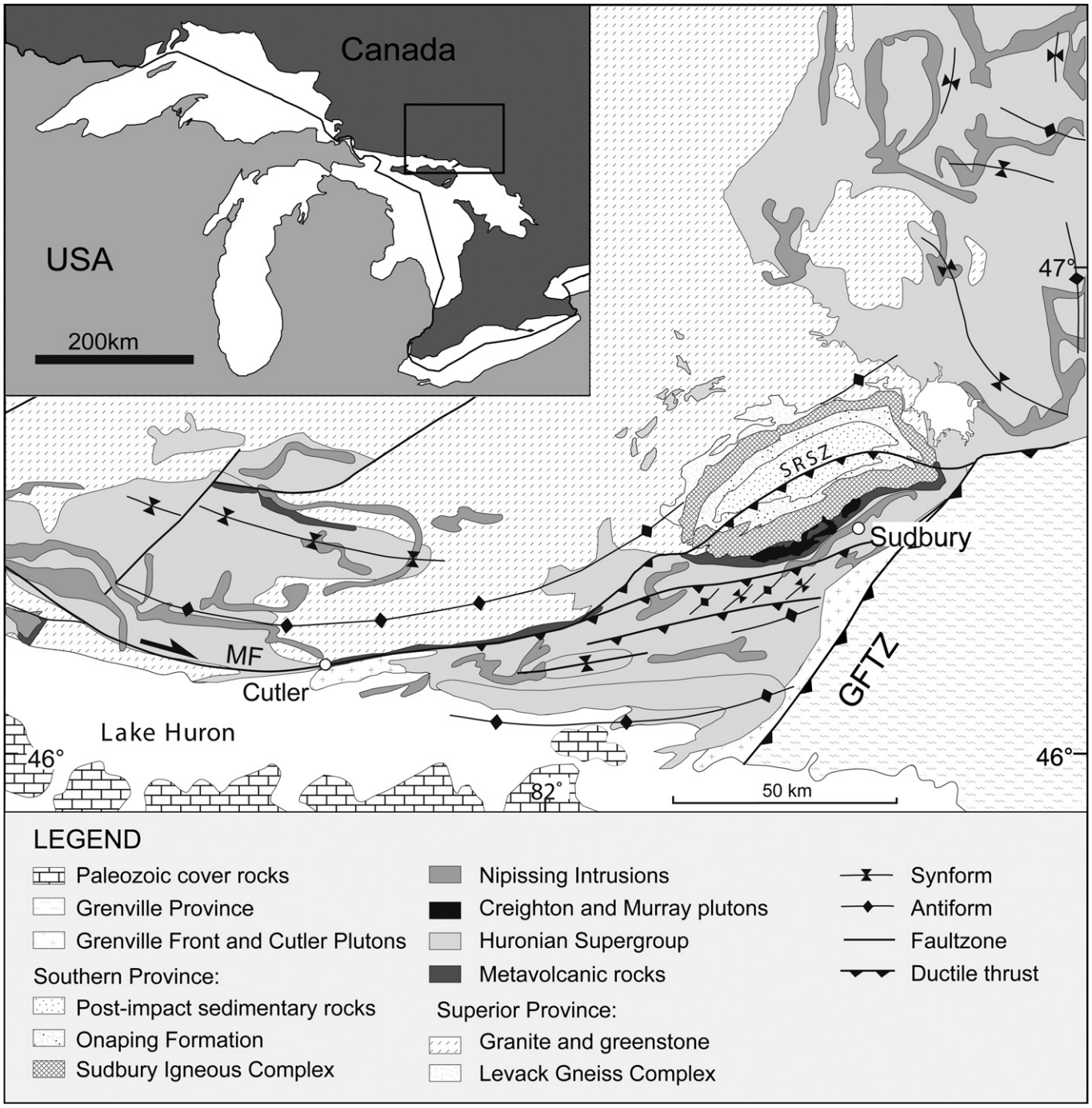

Fig. 1. Simplified tectonic map, modified from Card et al. (1984), showing the relics of the central Sudbury impact structure as part of the Eastern Penokean Orogen in the southern Canadian Shield. The Sudbury Igneous Complex rests on Archean rocks, notably granulites of the 2.7 Ga Levack Gneiss Complex in the north, and Paleoproterozoic rocks of the Huronian Supergroup in the south. SRSZ: South Range Shear Zone, GFTZ: Grenville Front Tectonic Zone, MF: Murray Fault.

Granophyre layers (Fig. 2: Grieve et al., 1991; Deutsch et al., 1995; Therriault et al., 2002), likely within about 10,000 years (Prevec and Cawthorn, 2002; Zieg and Marsh, 2005).

Based on impact models, the SIC formed in a large impact basin with a flat crater floor (e.g., Grieve et al., 1991; Deutsch et al., 1995; Ivanov and Deutsch, 1999). Its elliptical outline (Fig. 2), dip of lower contact toward the centre of the Sudbury Basin (Dressler, 1984a) and asymmetric deep structure (Milkereit et al., 1992) point to a synformal geometry of the melt sheet (Coleman, 1905, 1907; Collins and Kindle, 1935). The asymmetry of the SIC is attributed to northwest-directed displacement of the South Range on the South Range Shear Zone (Fig. 2), a prominent ductile thrust characterized by asymmetric mineral fabrics (Shanks and Schwerdtner, 1991). In reflection seismic profiles, the thrust is evident by imbricated contacts of the SIC and by southward inclined,

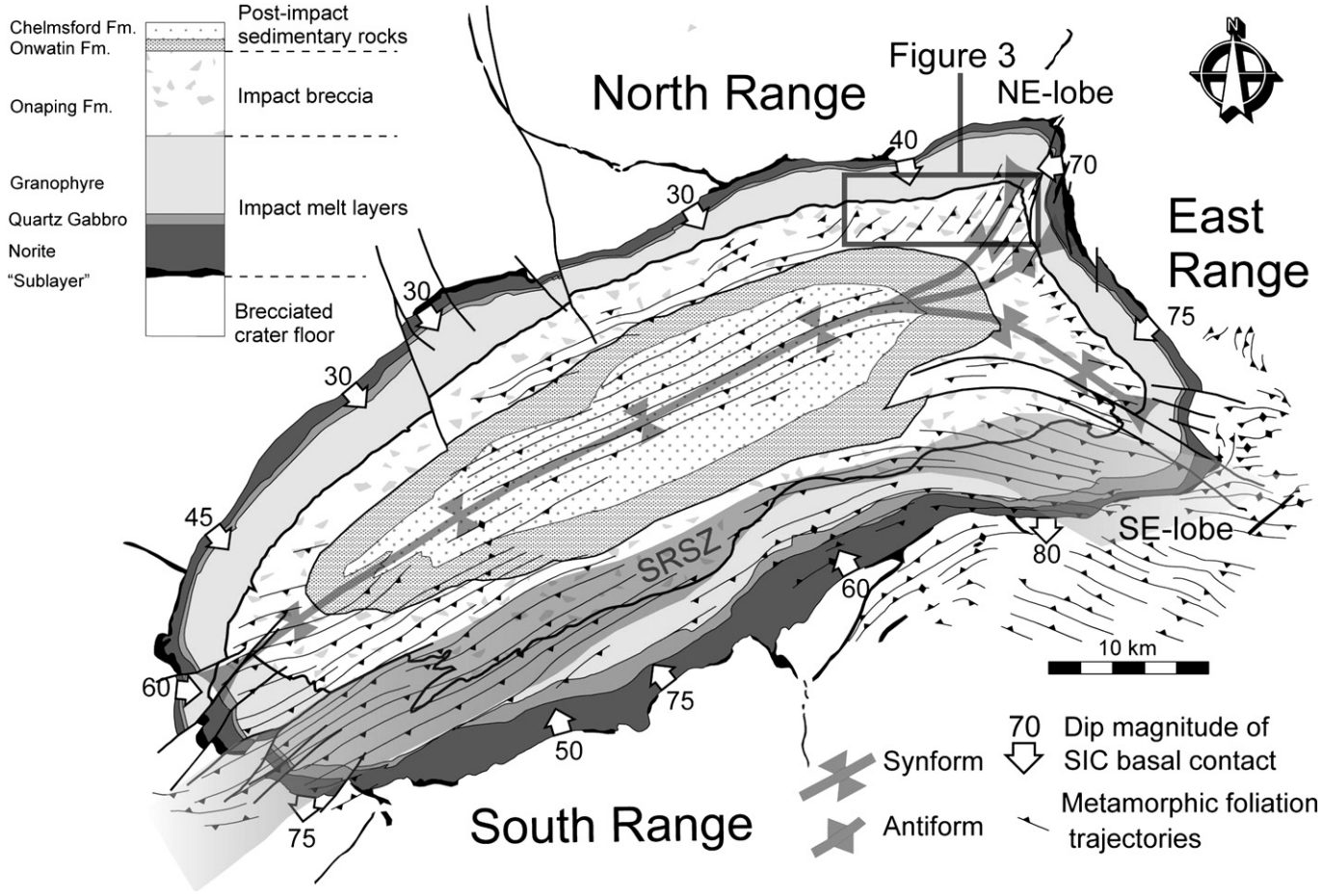

Fig. 2. Simplified geological map of the Sudbury Basin showing trajectories of post-impact planar metamorphic shape fabrics and the dips of the base of the SIC (modified from Cowan et al., 1999). Fold axes are from Riller (2005). SRSZ: South Range Shear Zone.

strong reflectors, interpreted as shear planes (Milkereit et al., 1992; Boerner et al., 2000). The South Range Shear Zone was active during the Penokean (Shanks and Schwerdtner, 1991; Riller et al., 1998) and Mazatzal-Labradorian (Bailey et al., 2004) Orogenies.

The South Range Shear Zone does, however, not account for the rather steep attitude and curvi-planar geometry of the lower contact of the SIC, notably in the East Range and the South Range (Fig. 2). This geometry has prompted a number of workers to regard the SIC as having acquired its shape by non-cylindrical folding after solidification (Grieve et al., 1991; Cowan and Schwerdtner, 1994; Deutsch et al., 1995) and is consistent with the NE and SE lobes and the overall structural continuity (Fig. 2). However, in contrast to the Onaping Formation and post-impact sedimentary rocks, the SIC is largely devoid of mesoscopic ductile strain fabrics (Fig. 2: Rousell, 1984; Muir and Peredery, 1984). This absence holds largely also for the two lobes of the SIC, where strains would be expected to be maximal, if the SIC acquired its shape by folding from a primary subhorizontal sheet geometry (Cowan, 1999; Cowan et al., 1999).

To investigate folding of the SIC, a detailed structural analysis was conducted of the Onaping Formation and upper Granophyre of the SIC in NE Sudbury Basin (Figs. 2 and 3a). The study area includes the inner arc of the NE-lobe and a significant portion of the moderately inclined North Range. Our objective was to document the geometry and scale of structures and their variation with lithology and distance to the NE-lobe (Fig. 3a). Lithological mapping, structural measurements at a total of 1300 stations, microstructural observations, a remote sensing study to identify prominent structural discontinuities and kinematic analysis of these discontinuities form the basis for our interpretation of the formation of the Sudbury Basin.

2. Lithological characteristics of the Onaping Formation

The Onaping Formation is an up to 2 km thick heterolithic breccia (Fig. 4) containing lithic and melt fragments (Muir and Peredery, 1984; Peredery and Morrison, 1984). The contact of the Onaping Formation with the Granophyre was found to be gradational over tens of meters in the NE-lobe. The contact to the overlying post-impact argillite and siltstone of the Onwatin Formation is not exposed in the study area but reported to be conformable (Rousell, 1984; Muir and Peredery, 1984).

The Onaping Formation consists of four subunits (Muir and Peredery, 1984) that are the Basal Member, the Grey Member, the Green Member and the Black Member, the contacts of

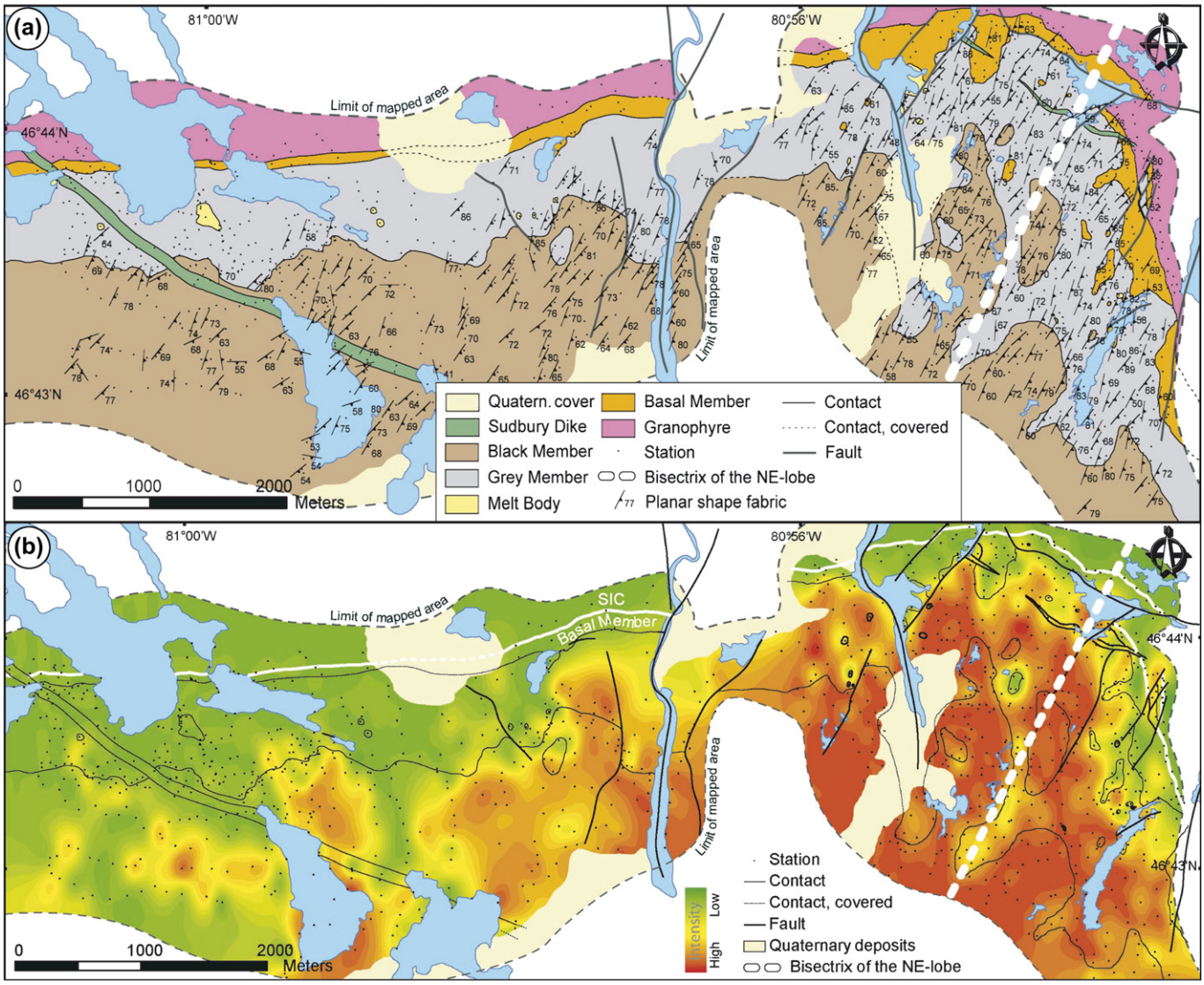

Fig. 3. Structure of the Onaping Formation in the NE-lobe of the SIC. (a) Geological map and orientation of planar metamorphic shape fabrics. Note the increase in undulations of lithological contacts culminating in poly-harmonic structural domes and basins in the Onaping Formation in the core of the NE-lobe. Also, the strike of inclined planar shape fabrics becomes more uniform, i.e., NE–SW, towards the bisectrix. (b) Estimates of mineral shape fabric intensity. Intensity increases toward upper stratigraphic levels of the Onaping Formation and toward the bisectrix of the NE-lobe.

which are gradational over tens of meters. Mapping of the Green Member (Avermann, 1999) was difficult in the study area as it could only be identified by thin-section analysis. It is, therefore, not considered in our study.

In the study area (Fig. 3a), the Basal Member is characterized by Archean and Proterozoic rock fragments, measuring generally 0.5–10 m in diameter, in an igneous-textured, granophyric matrix. Melt bodies, predominantly found at the interface of the Basal Member and the Grey Member (Fig. 3a), display crystalline cores and chilled margins with well-defined contacts to the host rock.

The Grey Member is lithologically heterogeneous with matrix variation from quartz-rich and fine-grained at the base to finer-grained and chlorite-rich near the top of the unit. Mafic minerals such as hornblende, biotite and chlorite are more abundant in the Grey Member than in the Basal Member. Fragments in the Grey Member consist of recrystallized quartz aggregates, sericitised feldspar crystals and sulphide minerals with resorbed boundaries (Fig. 4b).

The Black Member owes its colour to the dominant content of mafic matrix minerals, such as chlorite and epidote, and carbon particles. In general, the matrix of the Black Member is finer-grained than that of the Basal and Grey Members and is almost cryptocrystalline. Fragments include granitic and carbonaceous clasts as well as polycrystalline quartz and feldspar crystals (Figs. 4a and 5f).

3. First-order structure of the Onaping Formation

The NE-lobe is characterized by a pronounced curvature of the SIC in map view (Figs. 2 and 6). In the North Range, the basal SIC contact dips at 40° southward, whereas in the East

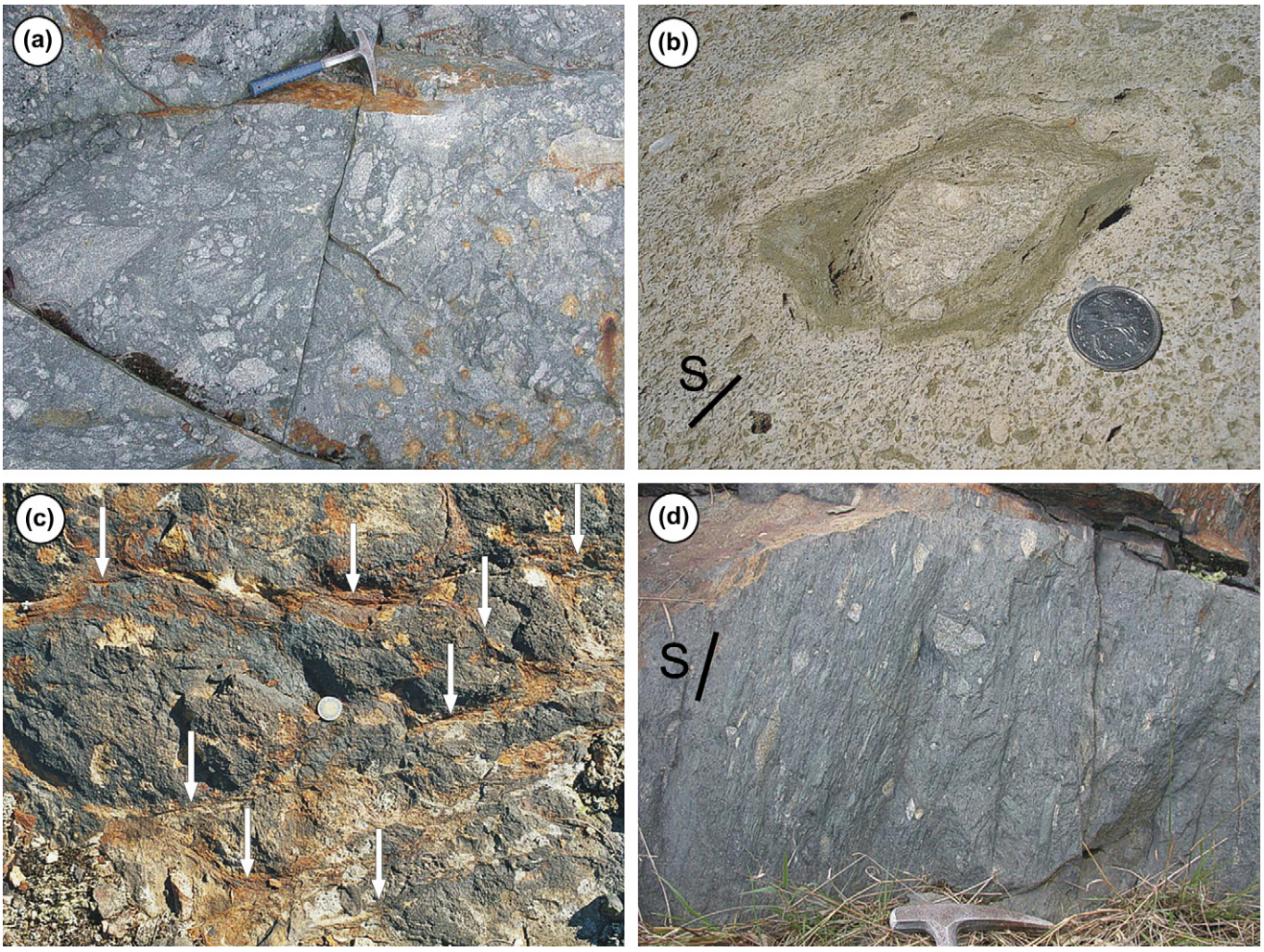

Fig. 4. Photos showing four levels of shape fabric intensity and petrographic characteristics and of the Onaping Formation. (a) Random distribution of angular, granitoid fragments in Black Member points to lack of strain. (b) Fragment with resorbed margin at the transition of Grey Member to Black Member. Weak shape-preferred orientation of small fragments in matrix defines low shape fabric intensity. (c) Localisation of strain in anastomosing shear zones (arrows) in Granophyre indicates moderate fabric intensity. (d) Pervasive mineral foliation in the matrix and highly stretched fragments is characteristic of strong fabric intensity. S in (b) and (d) denotes trace of foliation.

Range, it dips 70° toward the west (Fig. 2: Rousell, 1984). This amounts to an angle of 103° between both flanks of the SIC, whereby the bisector plane of the flanks dips at 70° towards the east–southeast (Fig. 7b).

The contacts between the individual members of the Onaping Formation and, to some extent also the contact between the Onaping Formation and the SIC, undulate throughout the Sudbury Basin (Dressler, 1984a). In the study area, contact undulations are well apparent and become more pronounced toward higher stratigraphic levels of the Onaping Formation and toward the trace of the bisector plane of the NE-lobe at surface, the bisectrix (Fig. 3a). Here, the units of the Onaping Formation are apparently thickened and highly lobate (Figs. 3a and 6).

Prominent structural discontinuities in the NE-lobe were identified by remote sensing analysis of monochrome aerial stereo photos, coloured, high-resolution digital aerial photos and a 30 m-resolution Shuttle Radar Topography Mission (SRTM) digital elevation model. First-order topographic lineaments were imaged by hill shade and slope maps of topography generated from SRTM data and by stereoscopical inspection of air photos (Fig. 8). The comparison of topographic lineaments with geological characteristics such as strike separations of lithological contacts revealed whether lineaments correspond to fault zones.

Based on preferred orientation, four sets of topographic lineaments were identified (Fig. 8). Set 1 consists of NW–SE trending lineaments that occur chiefly in the North Range SIC and adjacent Archean rocks that, in general, do not displace lithological contacts. This set correlates with diabase dikes of the ca. 1.2 Ga Sudbury dike swarm. As these dikes are less resistant to erosion than their more felsic host rocks, they form marked topographic depressions in the study area. Set 2 is made up of a few northerly trending lineaments west of the NE-lobe, which displace the contacts of the SIC.

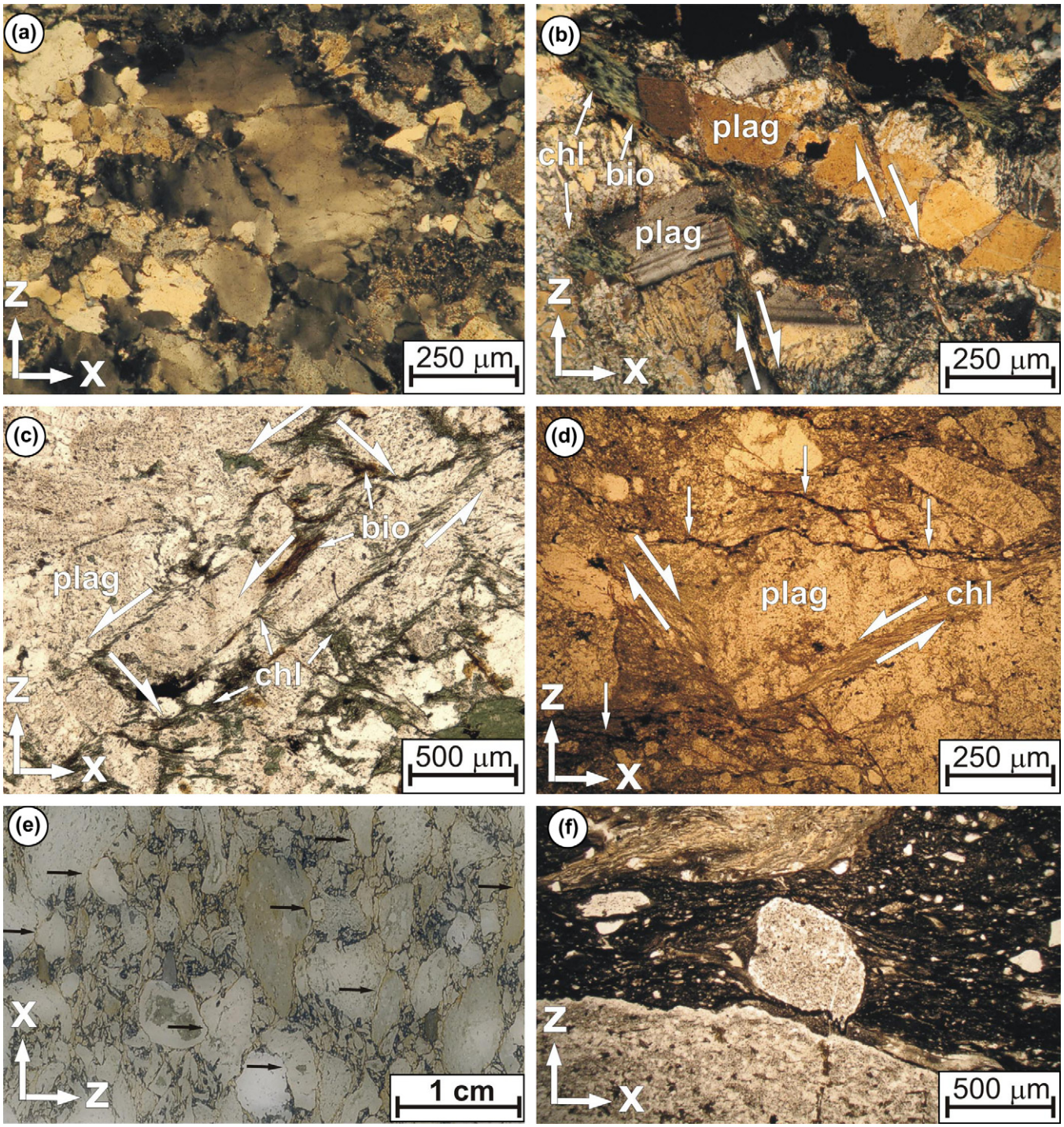

Fig. 5. Photomicrographs showing microstructural characteristics of the Onaping Formation and the Granophyre. (a) Serrated grain boundaries and subgrain formation in quartz of Basal Member (crossed polarised light). (b) Granophyre showing fractured plagioclase (plag). Note fibres of biotite (bio) and chlorite (chl) in shear fractures separating displaced plagioclase fragments. Relative sense of displacement is indicated by half arrows (crossed polarised light). (c) Conjugate shear fractures (half arrows) decorated by biotite (bio) and chlorite (chl) fibres in Granophyre (plane polarised light). (d) Grey Member showing pressure-solution seams characterized by opaque minerals (white arrows) and conjugate shear fractures denoted by half arrows (plane polarized light). (e) Impinging fragment boundaries (black arrows) in Black Member. (f) Black Member showing symmetric strain shadows of foliated chlorite matrix around polycrystalline quartz clast (plane polarized light). *X* and *Z* in all figures refer, respectively, to the long and short axes of the mineral fabric ellipsoid.

This set belongs to faults of the so-called Onaping system of the southern Canadian Shield, which is of minor structural importance in the Sudbury area (Rousell, 1984). Set 3 lineaments occur within the SIC of the NE-lobe and are parallel to its contacts, i.e., they mimic the curvature of the SIC. We were unable to resolve the origin of this lineament set. Finally, there is a set of lineaments, set 4, that occurs mostly in the Onaping Formation and Granophyre of the NE-lobe. Lineaments of this

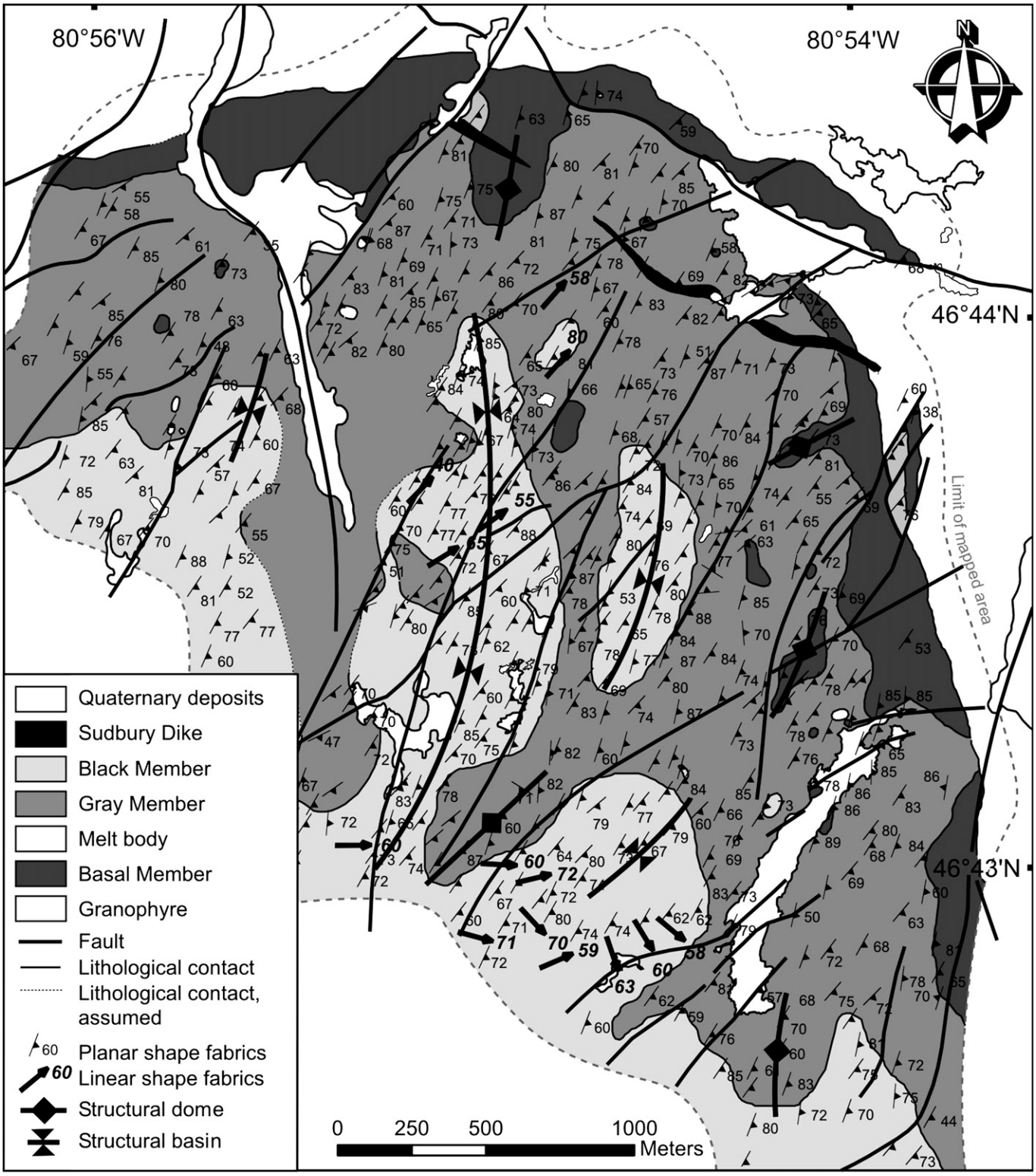

Fig. 6. Structural map of the NE-lobe showing the orientation of planar and linear mineral shape fabrics.

set are parallel to the bisectrix of the NE-lobe, displace the contact of the Onaping Formation with the Granophyre and thus, constitute faults. However, the strike separation on these faults is significantly smaller within the Onaping Formation, where the southern termini of the faults are generally ill-defined. This geometry applies particularly to the two most prominent faults east of the bisectrix, which displace the lower contact of the SIC by hundreds of meters.

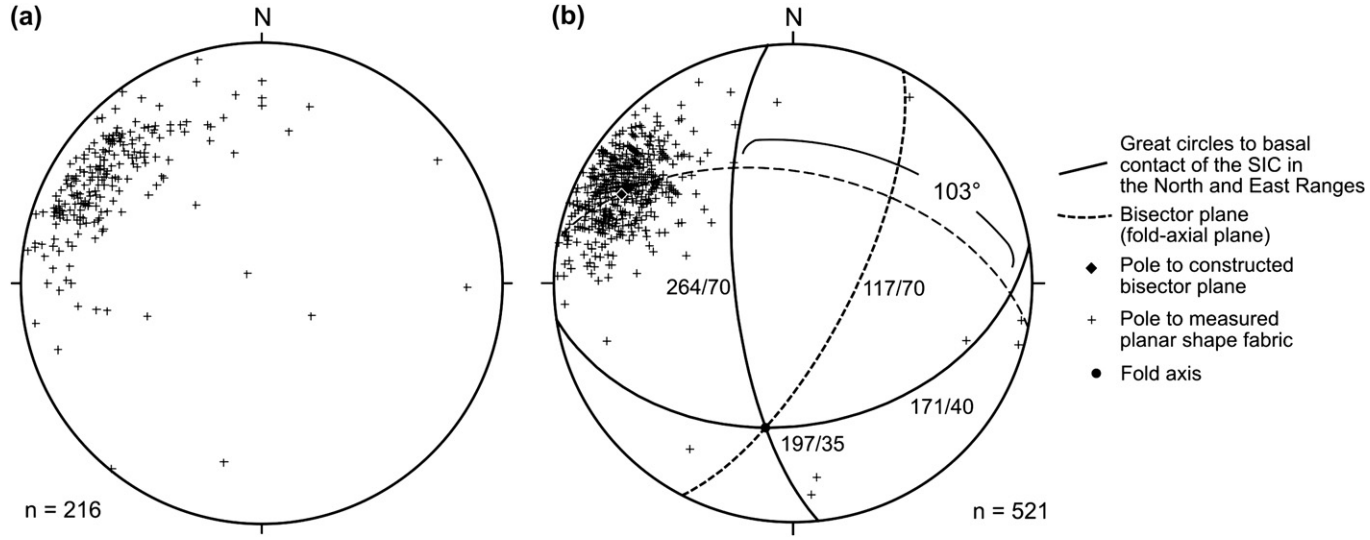

Fig. 7. Lower-hemisphere, equal-area projections of planar and linear structures from (a) west and (b) east of longitude 80°56′W in the study area (Fig. 3). In (b), measured poles to planar metamorphic shape fabrics cluster tighter around the pole to the bisector plane derived from the dip of the basal SIC contact.

4. Metamorphic conditions of mineral shape fabric formation

The Onaping Formation and post-impact sedimentary rocks were affected by lower greenschist-facies metamorphism (Card, 1978; Fleet et al., 1987). In the study area, metamorphic mineral shape fabrics appear in the Onaping Formation and to some degree also in the Granophyre (Fig. 3a). Metamorphic layering in the Onaping Formation is generally defined by the shape-preferred orientation of chlorite, quartz and epidote. Collectively, these minerals constitute the matrix and are formed from the chemical breakdown of plagioclase- and biotite-rich lithic fragments. Spacing of metamorphic layering decreases with increasing content of matrix minerals, notably of chlorite, and is developed best in the Black Member (Fig. 4d).

Metamorphic shape fabrics in the quartz–feldspar-rich Granophyre and the Basal Member are characterized by dynamic recrystallisation of quartz, evident by serrated grain boundaries and marginal subgrain formation (Fig. 5a). This points to temperatures above about 280 °C during crystal–plastic strain (Stipp et al., 2002). Plagioclase and K-feldspar crystals are not affected by dynamic recrystallisation but are fractured (Fig. 5b–d). Thus, temperature during deformation was below the minimum temperature for feldspar recrystallisation (450 °C: Fitz Gerald and Stünitz, 1993). Fibrous biotite and chlorite, formed in part from retrograde transformation of biotite, decorates the fractures between pulled-apart feldspar fragments (Fig. 5b–d). Relics of biotite fibres indicate that some deformation must have occurred at temperatures above the minimum temperature for metamorphic biotite growth (400 °C: Bucher and Frey, 2002, p. 232). Biotite–chlorite transformation occurs at temperatures below about 425 °C (Ferry, 1979). Thus, Granophyre and Basal Member deformed at temperatures between about 400 °C and 450 °C, followed by deformation under retrograde metamorphism.

Small-scale shear fractures in the Granophyre and the Basal Member form frequently conjugate sets (Fig. 5c, d). Shortening directions inferred from the local sense of displacement indicated by the geometry of fibrous biotite and chlorite is orthogonal to the metamorphic layering. In the Grey and Black Members, polycrystalline quartz porphyroclasts are enveloped by anastomosing discontinuities that formed perpendicular to the shortening direction and are marked by micaceous, oxide and opaque minerals (Fig. 5d) interpreted as residues of insoluble material. Toward the top of the Grey Member and in the Black Member, quartz fragments are largely devoid of intracrystalline plastic strain. Here, lithic fragments are characterized by impinging boundaries (Fig. 5e) and symmetric strain shadows filled with fibrous minerals that grew perpendicular to the shortening direction (Fig. 5f). Collectively, the microstructures in the Grey and Black Members indicate deformation by pressure solution chiefly of quartz fragments suggesting deformation temperatures below 300 °C (Passchier and Trouw, 1996, p. 48).

The Granophyre, the Basal Member and the lower portion of the Grey Member are more affected by discontinuous deformation, whereas the top of the Grey Member and the Black Member deformed chiefly by continuous flow on the thin-section scale. These mechanical differences are controlled by the primary fragment–matrix ratio as well as content and fabric of feldspar crystals rather than temperature. Specifically, low content of matrix minerals, high feldspar content and interlocking feldspar fabric in the Granophyre and Basal Member (Fig. 5b–d) caused these units to deform more discontinuously than the Grey and Black Members (Fig. 5f), although deformation temperatures of the latter were lower.

5. Geometry and intensity of mineral shape fabrics

Metamorphic shape fabrics in the study area are pervasively planar (S), in places linear–planar (L–S), notably near prominent faults (Fig. 6), whereby planar fabrics dip uniformly

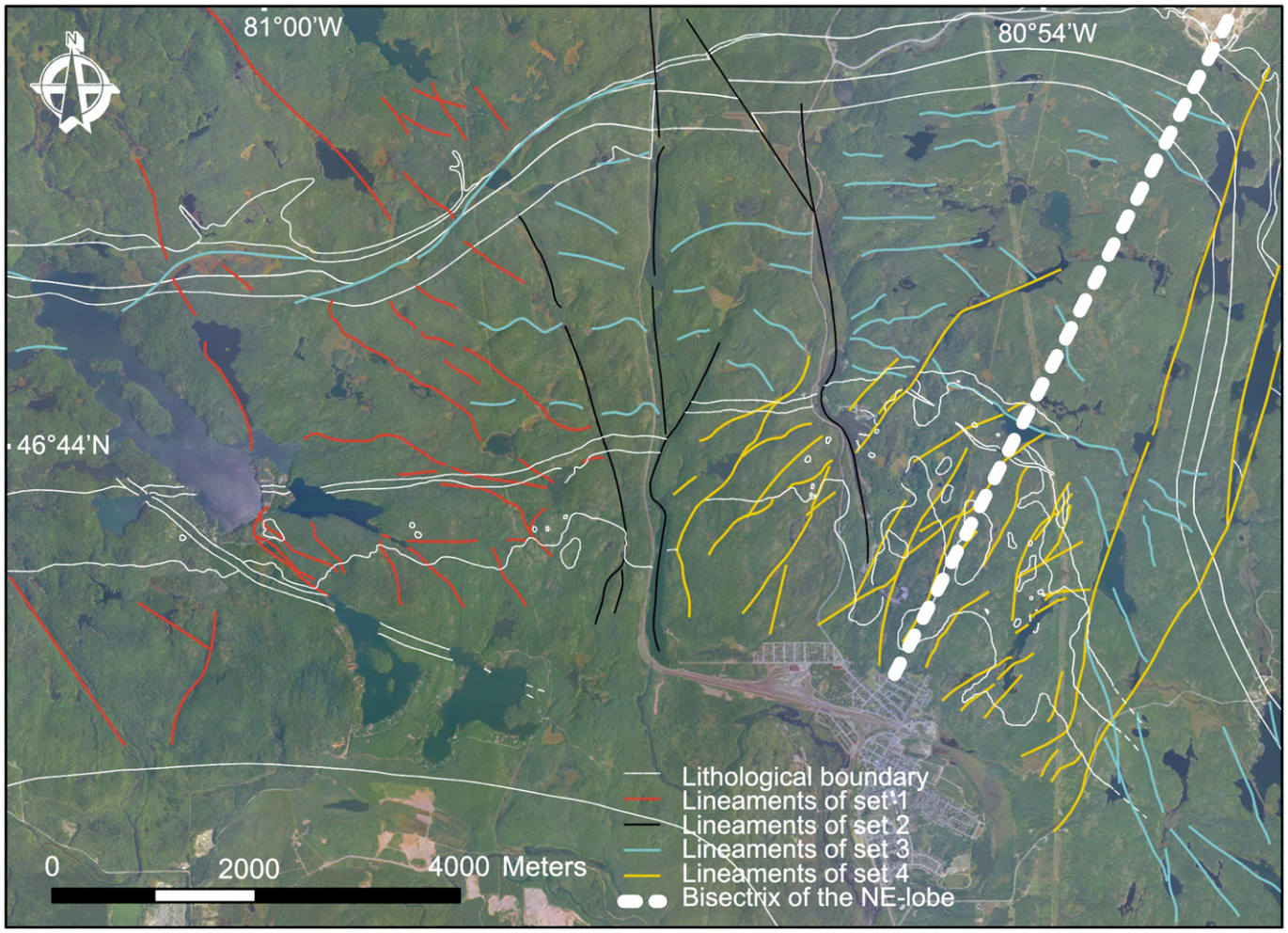

Fig. 8. Prominent topographic lineaments inferred from remote sensing analysis of the NE-lobe and superimposed on an aerial photo. Lineaments in the Onaping Formation transect poly-harmonic domes and basins and are sub-parallel to the trace of the bisector plane.

toward the southeast (Figs. 3a, 6 and 7). As mentioned beforehand, planar mineral fabrics are generally better developed at higher stratigraphic levels, notably in the phyllosilicate-rich Black Member (Figs. 3a, 4d and 5f). Only close to the bisectrix of the NE-lobe are mineral fabrics developed pervasively in the Grey Member, the Basal Member and sporadically in the Granophyre (Fig. 6), which is devoid of mesoscopic ductile strain elsewhere. Furthermore, the strike of planar shape fabrics becomes more uniform in orientation, i.e., NE–SW, with proximity to the bisectrix of the NE-lobe (Fig. 3a). This is also evident from the poles to planar fabrics, which cluster more closely around the pole to the bisector plane in the eastern portion (Fig. 7b), than they do in the western portion (Fig. 7a) of the study area.

Knowledge of fabric intensity and its spatial variation can be valuable to assess mechanisms and kinematics of deformed geological terranes. Based on the shape-preferred alignment of metamorphic minerals, localisation of ductile strain and ellipticity of fragments, fabric intensity was visually estimated at 1300 stations in the Onaping Formation and adjacent SIC (Fig. 3b). For this purpose, four levels of shape fabric intensity, encompassing unstrained and weakly, moderately as well as strongly deformed (Fig. 4), were distinguished by visual inspection in the field, akin to fabric intensity estimates in granitoid rocks (Riller and Schwerdtner, 1997). The spatial distributions of these four levels of fabric intensity (Fig. 3b) were statistically defined, using the Kriging method (Klimczak, 2006).

Similar to the variation in planar mineral fabric orientation, fabric intensity increases toward upper stratigraphic levels of the Onaping Formation and, more importantly, toward the bisectrix of the NE-lobe (Fig. 3b). This suggests that gradients in mineral fabric intensity are controlled by lithology and strain, respectively. Based on the concordance of planar fabrics and the bisector plane, we interpret the mineral fabrics as axial-planar fabrics and, consequently, the bisector plane as a fold-axial plane. This structural geometry and the increase in fabric intensity toward the NE-lobe are consistent with folding of the Onaping Formation around a moderately south–southwest plunging fold axis (Fig. 7b). Dip decrease of the units toward the fold axis accounts for their apparent thickening in the NE-lobe constituting a kilometre-scale fold (Figs. 3a

and 7b). Moreover, distortion of strata in the inner arc of this fold suggests that the lobes and map-view inclusions of one Member within another represent higher-order, open and non-cylindrical folds, i.e., elongate structural domes and basins (Fig. 6).

6. Kinematic analysis of prominent discontinuities

On the local scale, strains are greater near prominent set 4 faults in the Onaping Formation, particularly at their ill-defined southwestern termini. Moreover, shape fabrics with L–S geometry were found only at prominent faults (Fig. 6) suggesting that these fabrics developed during fault activity. This relationship can be used to determine the sense of displacement on prominent faults in the core of the NE-lobe.

Schwerdtner (1998) developed a simple graphical method, which determines the local sense-of-shear strain components using mineral shape fabrics as indicators of finite strain. The method can be applied to various tectonic settings, including transpressive deformation and oblique thrusting, and is particularly useful for determining the range of possible tangential shear strain vectors (γ), i.e., the sense-of-shear, of kilometre-scale shear belts (Schwerdtner et al., 2005). The technique relies on the knowledge of the orientation of the shear plane or fault zone, i.e., a lithotectonic boundary (LTB), and associated L–S mineral shape fabrics (Fig. 9). As these quantities are known from the core of the NE-lobe, this technique may be used to determine the sense of displacement on set 4 faults.

It is generally possible to split the resultant shear strain vector into two oblique vectors γX and γZ. The two vectors parallel, respectively, the orthogonal projection of the lineation direction (X) and the orthogonal projection of the foliation normal (Z), onto the tangent plane to a high-strain-zone segment or its concordant fault (''LTB'' in Fig. 9). The magnitude of the two vectors is generally unknown, but one may plot their directions on the upward facing side of the tangent plane to the high-strain zone (Fig. 9). The possible range of shear strain directions lies in the acute angle between γX and γZ (Fig. 9b, c), from which the range of possible shortening directions may be inferred (Schwerdtner, 1998).

Kinematic analysis using the method by Schwerdtner (1998) was conducted at seven stations located at prominent set 4 faults in the Onaping Formation of the NE-lobe (Fig. 10). Based on drill core analysis, the fault planes (i.e., LTBs) dip at about 80° towards the NW (personal communication with staff geologists of INCO Ltd. and Falconbridge Ltd). Geometrically, the mineral shape fabric axes, fault orientation and inferred range of shear strain directions indicate overall NW over SE sense-of-shear on the faults (Fig. 10b). Thus, the North Range was translated over the East Range on the faults in this area.

In addition to reverse sense-of-shear, a conspicuous pattern in horizontal shear components and respective directions of horizontal shortening is inferred from the kinematic analysis. North of the bisectrix (stations 1–3), a pronounced sinistral shear component is evident (Fig. 10b). By contrast, south of the bisectrix (stations 5–7) a dextral shear component prevails (Fig. 10b). At station 4, located on the bisectrix, the component of horizontal shear is inconclusive. Accordingly, inferred local shortening directions are N–S north of the bisectrix, NW–SE at the bisectrix and WNW–ESE south of the bisectrix (Fig. 10). The pattern of horizontal shear and local shortening directions indicate differential shear on prominent discontinuities separating elongate zones in the Onaping Formation of the NE-lobe. This pattern may be interpreted in terms of passive folding (Twiss and Moores, 1992, Chapter 12) of the Onaping Formation in the inner arc of the lobe.

7. Deformation of the Onaping Formation by folding

The formation of higher-order, poly-harmonic folds of mechanically less competent materials in the cores of mechanically stronger lithological units forming lower-order buckle

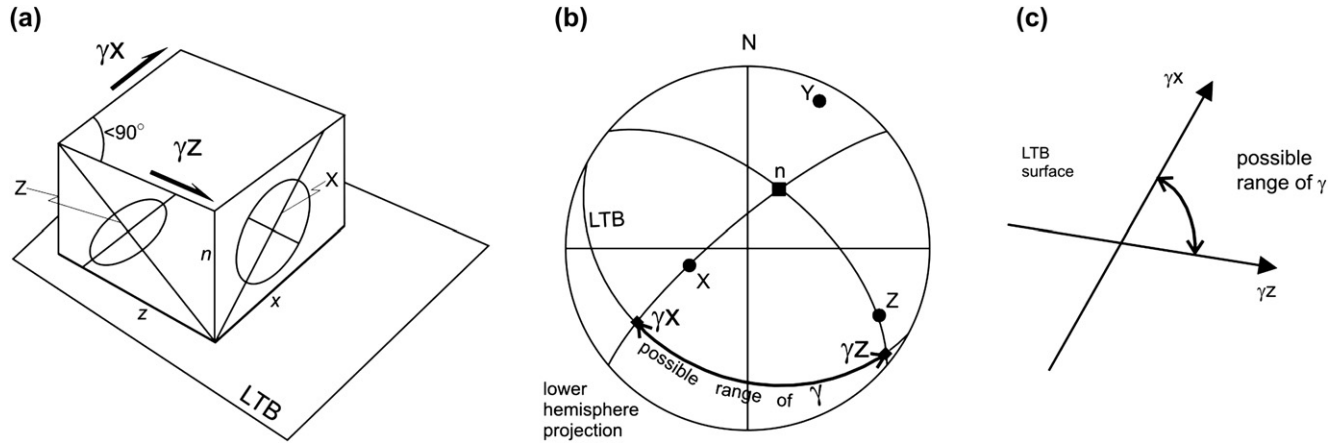

Fig. 9. Determination of the direction of the shear strain γ on a lithotectonic boundary (LTB) with normal n, using a hypothetical L–S shape fabric. The lineation direction (L) is parallel to the X-axis, and the Z-axis is normal to foliation plane (S). The smaller the angle between γX and γZ, the closer is the approximation of the γ direction. (a) Schematic block diagram depicting the geometric relationship between fabric quantities. (b) Graphical derivation of the possible range of shear strain directions in a lower-hemisphere equal-area projection. (c) The shear strain γ lies in the acute angle defined by γX and γZ on the LTB.

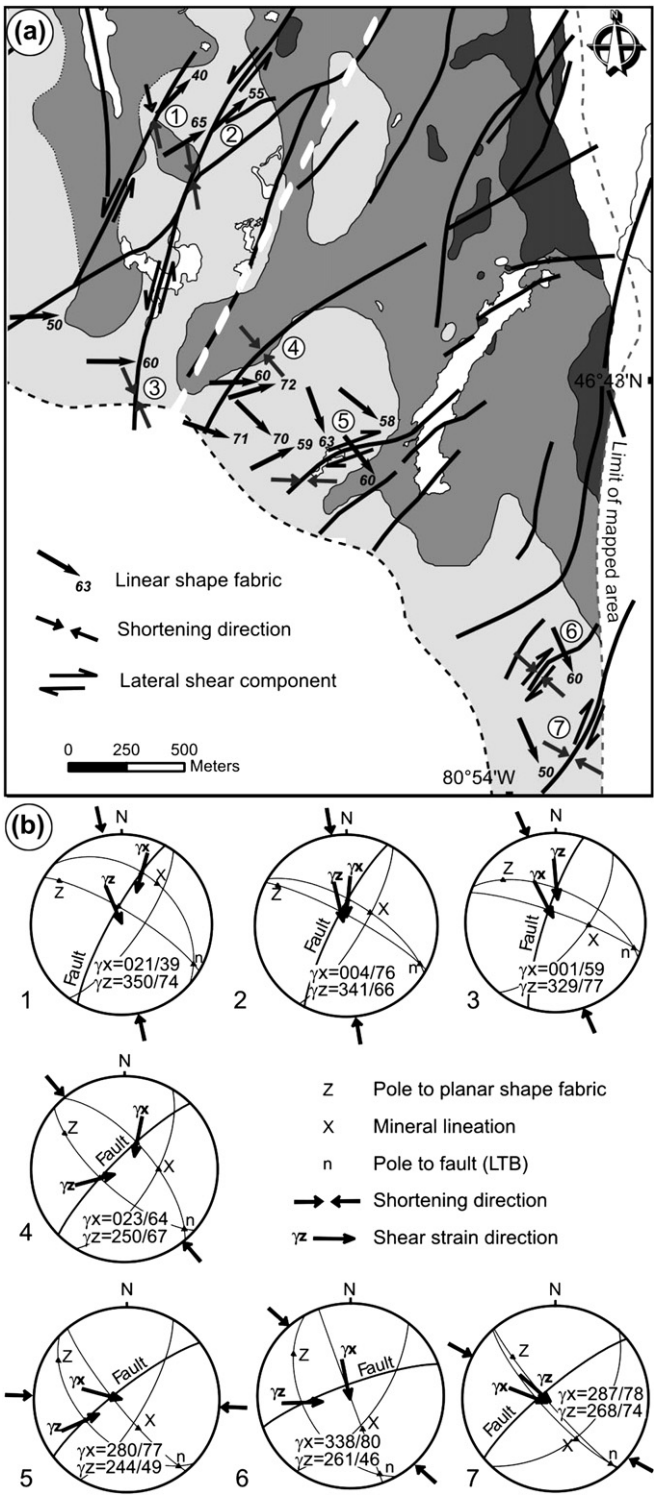

Fig. 10. Kinematics of prominent discontinuities in the Onaping Formation of the NE-lobe. (a) Map showing the horizontal components of relative displacement on oblique reverse faults and inferred shortening directions using the method by Schwerdtner (1998). Note the variation in horizontal shear components, i.e., left-lateral in the northwest and right-lateral in the southeast of the bisectrix. Patterns of geological units are the same as in Fig. 6. (b) Graphic derivation of the sense-of-shear on prominent dislocations and inferred directions of shortening from selected areas. For explanation of constructions refer to text.

folds is a common characteristic for fold-adjustment flow (Schwerdtner and Van Berkel, 1991). Accordingly, we interpret open, structural domes and basins in the mechanically weaker Grey and Black Members and thickening of these units in the NE-lobe to have formed by fold-adjustment flow controlled by deformation of the mechanically stronger Granophyre and Basal Member.

Microfabrics indicate that the maximum temperatures recorded during deformation in the Black and Grey Members are lower (<300 °C) than in the Basal Member and the Granophyre (between 400 °C and 450 °C). This holds also for Archean granitoid rocks underlying the NE-lobe, characterized by brittle deformation and lack of pervasive post-impact ductile strain (Doman and Riller, 2007). Thus, temperature during post-impact deformation decreased away from the Basal Member, i.e., stratigraphically downward and upward. This temperature variation within the Onaping Formation and underlying rock units is difficult to reconcile with regional deformation and metamorphism due to burial of the units. It is, however, consistent with isobaric cooling of the impact melt sheet and the Onaping Formation (e.g., Zieg and Marsh, 2005). We, therefore, advocate fabric development and, thus, initial folding of the Onaping Formation during cooling but after solidification of the impact melt sheet, more specifically, upon reaching middle greenschist-facies metamorphic conditions (see also Riller, 2005).

8. Conclusions

Structural analysis of the Onaping Formation aided in understanding better the mechanism and age of folding strain that contributed to the formation of the Sudbury Basin. Our analysis shows that fabric development in the Onaping Formation was controlled by lithology, temperature gradients and proximity to the bisectrix of the NE-lobe of the Basin. The (1) presence of open structural domes and basins, (2) progressive alignment of planar mineral shape fabrics toward axial-planar geometry, (3) increase in shape fabric intensity towards the bisectrix and (4) kinematics of prominent set 4 faults are, collectively, compatible with folding of the Onaping on the kilometre scale. Thereby, the bisectrix constitutes the trace of the fold-axial plane. As this plane is inferred from the dips of the lower contacts of the SIC, and set 4 faults affected also the Granophyre, the SIC must have participated in this deformation. Open structural domes and basins in the mechanically weaker upper members of the Onaping Formation are interpreted to have formed as a result of fold-adjustment flow during deformation of the mechanically stronger SIC. Deformation during cooling of the SIC and the Onaping Formation accounts for the observed microstructural characteristics in these units, i.e., deformation by pressure solution in the Black and Grey Members and crystal–plastic strain in quartz in the Basal Member and the Granophyre. Thus, formation of the Sudbury Basin may have started as early as middle greenschist-facies metamorphic conditions were reached upon cooling of the superheated melt sheet.

Acknowledgements

This work was supported by the German Science Foundation (grant Ri 916/5) as part of the Priority Program "International Continental Scientific Drilling Program". Logistical support by Wallbridge Mining Ltd., Lively, Ontario, is greatly appreciated. Falconbridge Ltd. and INCO Ltd., Sudbury, Ontario, are thanked for permitting access to their properties. The manuscript benefited greatly from reviews by Declan de Paor, John Spray and William Dunne.

References

Avermann, M.E., 1999. The Green Member of the Onaping Formation, the collapsed fireball layer of the Sudbury impact structure, Ontario, Canada. In: Dressler, B.O., Sharpton, V.L. (Eds.), Large Meteorite Impacts and Planetary Evolution II, Geological Society of America Special Paper, vol. 339, pp. 323–330.

Bailey, J., Lafrance, B., McDonald, A.M., Fedorowich, J.S., Kamo, S., Archibald, D.A., 2004. Mazatzal–Labradorian-age (1.7–1.6 Ga) ductile deformation of the South Range Sudbury impact structure at the Thayer Lindsley mine, Ontario. Canadian Journal of Earth Sciences 41, 1492–1505.

Boerner, D.E., Milkereit, B., Wu, J., Salisbury, M., 2000. Seismic images and three-dimensional architecture of a Proterozoic shear zone in the Sudbury structure (Superior Province, Canada). Tectonics 19, 397–405.

Bray, J.G., Geological staff, 1966. Shatter cones at Sudbury. Journal of Geology 74, 243–245.

Brocoum, S.J., Dalziel, I.W.D., 1974. The Sudbury Basin, Southern Province, Grenville Front, and the Penokean Orogeny. Geological Society of America Bulletin 85, 1571–1580.

Bucher, K., Frey, M., 2002. Petrogenesis of Metamorphic Rocks. Springer-Verlag, Berlin, Heidelberg.

Card, K.D., 1978. Metamorphism in middle Precambrian (Aphebian) rocks of the eastern Southern Province. In: Fraser, J.A., Heywood, W.W. (Eds.), Metamorphism in the Canadian Shield, Geological Survey of Canada Paper, 78-10, pp. 269–282.

Card, K.D., Gupta, V.K., McGrath, P.H., Grant, F.S., 1984. The Sudbury Structure: its regional geological and geophysical setting. In: Pye, E.G., Naldrett, A.J., Giblin, P.E. (Eds.), The Geology and Ore Deposits of the Sudbury Structure, Special Publication, vol. 1. Ontario Geological Survey, Toronto, pp. 25–44.

Coleman, A.P., 1905. The Sudbury Nickel region. Ontario Bureau of Mines Annual Report 14 (3), 1–188.

Coleman, A.P., 1907. The Sudbury laccolith sheet. Journal of Geology 15, 759–782.

Collins, W.H., Kindle, E.D., 1935. Life history of the Sudbury Nickel Irruptive. Part II. Intrusion and deformation. Transactions of the Royal Society of Canada 29, 27–47.

Cowan, E.J., 1999. Magnetic fabric constraints on the initial geometry of the Sudbury Igneous Complex: a folded sheet or a basin-shaped igneous body? Tectonophysics 307, 135–162.

Cowan, E.J., Riller, U., Schwerdtner, W.M., 1999. Emplacement geometry of the Sudbury Igneous Complex: structural examination of a proposed impact melt-sheet. In: Dressler, B.O., Sharpton, V.L. (Eds.), Large Meteorite Impacts and Planetary Evolution II, Geological Society of America Special Paper, vol. 339, pp. 399–418.

Cowan, E.J., Schwerdtner, W.M., 1994. Fold origin of the Sudbury Basin. In: Ontario Geological Survey Special Paper, vol. 5, 45–55.

Deutsch, A., Grieve, R.A.F., Avermann, M., Bischoff, L., Brockmeyer, P., Buhl, D., Lakomy, R., Müller-Mohr, V., Ostermann, M., Stöffler, D., 1995. The Sudbury Structure (Ontario, Canada): a tectonically deformed multi-ring basin. Geologische Rundschau 84, 697–709.

Doman, D., Riller, U., 2007. The importance of discontinuous deformation in the eastern Sudbury Igneous Complex. Geophysical Research Abstracts 9, 10220.

Dressler, B.O., 1984a. General geology of the Sudbury Structure. In: Pye, E.G., Naldrett, A.J., Giblin, P.E. (Eds.), The Geology and Ore Deposits of the Sudbury Structure, Special Publication, vol. 1. Ontario Geological Survey, Toronto, pp. 57–82.

Dressler, B.O., 1984b. The effects of the Sudbury event and the intrusion of the Sudbury Igneous Complex on the footwall rocks of the Sudbury structure. In: Pye, E.G., Naldrett, A.J., Giblin, P.E. (Eds.), The Geology and Ore Deposits of the Sudbury Structure, Special Publication, vol. 1. Ontario Geological Survey, Toronto, pp. 97–136.

Ferry, J.M., 1979. Reaction mechanisms, physical conditions, and mass transfer during hydrothermal alteration of mica and feldspar in granitic rocks from south-central Maine, USA. Contributions to Mineralogy and Petrology 68, 125–139.

Fitz Gerald, J.D., Stünitz, H., 1993. Deformation of granitoids at low metamorphic grades. I. Reactions and grain size reduction. Tectonophysics 221, 269–297.

Fleet, M.E., Barnett, R.R., Morris, W.A., 1987. Prograde metamorphism of the Sudbury Igneous Complex. Canadian Mineralogist 25, 499–514.

Grieve, R.A.F., Stöffler, D., Deutsch, A., 1991. The Sudbury Structure: controversial or misunderstood? Journal of Geophysical Research 96, 22753–22764.

Ivanov, B.A., Deutsch, A., 1999. Sudbury impact event: cratering mechanics and thermal history. In: Dressler, B.O., Sharpton, V.L. (Eds.), Large Meteorite Impacts and Planetary Evolution II, Geological Society of America Special Paper, vol. 339, pp. 389–397.

Klimczak, C., 2006. Deformation of the Onaping Formation in the NE-lobe of the Sudbury Igneous Complex, Ontario, Canada. Unpublished Diploma thesis. Free University Berlin, Germany, 72 pp.

Krogh, T.W., McNutt, R.H., Davis, G.L., 1982. Two high-precision U–Pb zircon ages for the Sudbury Nickel Irruptive. Canadian Journal of Earth Sciences 19, 723–728.

Krogh, T.E., Davis, D.W., Corfu, F., 1984. Precise U–Pb Zircon and Baddeleyite ages for the Sudbury area. In: Pye, E.G., Naldrett, A.J., Giblin, P.E. (Eds.), The Geology and Ore Deposits of the Sudbury Structure, Special Publication, vol. 1. Ontario Geological Survey, Toronto, pp. 431–446.

Milkereit, B., Green, A.21 others, 1992. Deep geometry of the Sudbury structure from seismic reflection profiling. Geology 20, 807–811.

Muir, T.L., Peredery, W.V., 1984. The Onaping Formation. In: Pye, E.G., Naldrett, A.J., Giblin, P.E. (Eds.), The Geology and Ore Deposits of the Sudbury Structure, Special Publication, vol. 1. Ontario Geological Survey, Toronto, pp. 139–210.

Passchier, C.W., Trouw, R.A.J., 1996. Microtectonics. Springer-Verlag, Berlin, Heidelberg, 289 pp.

Peredery, W.V., Morrison, G.G., 1984. Discussion of the origin of the Sudbury structure. In: Pye, E.G., Naldrett, A.J., Giblin, P.E. (Eds.), The Geology and Ore Deposits of the Sudbury Structure, Special Publication, vol. 1. Ontario Geological Survey, Toronto, pp. 491–512.

Prevec, S.A., Cawthorn, R.G., 2002. Thermal evolution and interaction between impact melt sheet and footwall: a genetic model for the contact sublayer of the Sudbury Igneous Complex, Canada. Journal of Geophysical Research 107, 2176, doi:10.1029/2001JB000525.

Riller, U., 2005. Structural characteristics of the Sudbury impact structure, Canada: impact-induced versus orogenic deformation – a review. Meteoritics & Planetary Science 40 (11), 1723–1740.

Riller, U., Schwerdtner, W.M., 1997. Mid-crustal deformation at the southern flank of the Sudbury Basin, central Ontario, Canada. Geological Society of America Bulletin 109, 841–854.

Riller, U., Schwerdtner, W.M., Robin, P.-Y.F., 1998. Low-temperature deformation mechanisms at a lithotectonic interface near the Sudbury Basin, Eastern Penokean Orogen, Canada. Tectonophysics 287, 59–75.

Riller, U., Schwerdtner, W.M., Halls, H.C., Card, K.D., 1999. Transpressive tectonism in the eastern Penokean orogen, Canada: consequences for Proterozoic crustal kinematics and continental fragmentation. Precambrian Research 93, 51–70.

Rousell, D.H., 1984. Structural geology of the Sudbury basin. In: Pye, E.G., Naldrett, A.J., Giblin, P.E. (Eds.), The Geology and Ore Deposits of the Sudbury Structure, Special Publication, vol. 1. Ontario Geological Survey, Toronto, pp. 83–95.

Schwerdtner, W.M., 1998. Graphic derivation of the local sense of shear of shear strain components in stretched walls of lithotectonic boundaries. Journal of Structural Geology 20, 957–967.

Schwerdtner, W.M., Van Berkel, J.T., 1991. The origin of fold abutments in the map pattern of the westernmost Grenville Province, central Ontario. Precambrian Research 49, 39–59.

Schwerdtner, W.M., Riller, U., Borowik, A., 2005. Structural testing of tectonic hypotheses by field-based analysis of distributed tangential shear: concrete examples from major high-strain zones in the Grenville Province and other parts of the southern Canadian Shield. Canadian Journal of Earth Sciences 42, 1905–1925.

Shanks, W.S., Schwerdtner, W.M., 1991. Structural analysis of the central and southwestern Sudbury Structure, Southern Province, Canadian Shield. Canadian Journal of Earth Sciences 28, 411–430.

Spray, J.G., Thompson, L.M., 1995. Friction melt distribution in a multi-ring impact basin. Nature 373, 130–132.

Spray, J.G., Butler, H.R., Thompson, L.M., 2004. Tectonic influences on the morphometry of the Sudbury impact structure: Implications for terrestrial cratering and modeling. Meteoritics & Planetary Science 39, 287–301.

Stipp, M., Stünitz, H., Heilbronner, R., Schmid, S., 2002. The eastern Tonale fault zone: a 'natural laboratory' for crystal plastic deformation of quartz over a temperature range from 250 to 700 °C. Journal of Structural Geology 24, 1861–1884.

Therriault, A.M., Fowler, A.D., Grieve, R.A.F., 2002. The Sudbury Igneous Complex, a differentiated impact melt sheet. Economic Geology 97, 1521–1540.

Twiss, R.J., Moores, E.M., 1992. Structural Geology. W.H. Freeman and Company, N.Y., 532 pp.

Zieg, M.J., Marsh, B.D., 2005. The Sudbury Igneous Complex: viscous emulsion differentiation of a superheated impact melt sheet. Geological Society of American Bulletin 117, 1427–1450.